

PHYSICAL REVIEW B

CONDENSED MATTER

THIRD SERIES, VOLUME 40, NUMBER 3

15 JULY 1989-II

Electronic structure, optical and magnetic properties of fcc palladium

H. Chen, N. E. Brener, and J. Callaway

Department of Physics and Astronomy, Louisiana State University, Baton Rouge, Louisiana 70803-4001

(Received 9 January 1989)

We report a self-consistent, all-electron, local-density-functional study of the electronic structure of paramagnetic fcc palladium. The linear combination of Gaussian orbitals method has been used. Associated with the band structure, we also present our results obtained for the density of states, Fermi surface, x-ray form factors, Compton profiles, and optical conductivity. In addition, we have investigated the magnetic-moment formation at expanded lattice constant by performing spin-polarized calculations. Our results are compared with experiments and with other calculations where possible.

I. INTRODUCTION

The electronic structure of palladium has probably been the most thoroughly studied of all the $4d$ transition metals. Its band structure has been reported by many authors.¹⁻⁷ However, many related properties such as the charge and momentum density and the optical conductivity, which are, in principle, rather easily obtained from the band structure and wave functions, have not been investigated as extensively. In the present work, all these quantities are obtained from an all-electron self-consistent calculation.

Early non-self-consistent calculations were all performed using the augmented-plane-wave (APW) method.¹⁻³ Using the relativistic APW method (RAPW), Anderson¹ computed the Fermi surface, density of states, and electronic specific-heat coefficients for palladium. A similar investigation was done by Mueller *et al.*,² also based on APW plus an interpolation scheme including relativistic corrections. Christensen³ used the same muffin-tin potential as Anderson's and calculated the density of states, joint density of states, the imaginary part of the dielectric function, and photoemission spectra. However, his work did not include the calculation of matrix elements. Among self-consistent calculations, a RAPW energy-band calculation was reported by MacDonald *et al.*⁴ They have mainly considered such properties as the Fermi surface and density of states which are directly related to the energy-band structure. Another self-consistent band calculation is due to Moruzzi *et al.*⁵ who used the Korringa-Kohn-Rostoker (KKR) method. To some degree, the band calculations mentioned above all involve the so-called muffin-tin shape approximations. Two other recent calculations have used localized orbitals

(LCAO) method⁷ or the mixed basis with pseudopotential method.⁶ However, these authors did not report any detailed studies of energy-band-related properties.

In this paper we present self-consistent, all-electron energy-band calculations for fcc palladium based on the local-density-functional approximation. We emphasize the following. (1) We have used the linear combination of Gaussian orbitals (LCGO) method which makes no shape approximations to charge densities and potentials. (2) Since matrix elements involving Gaussian orbitals can be very easily evaluated analytically, we have studied a variety of properties of Pd by explicitly evaluating matrix elements using self-consistent wave functions. Specifically, we have computed the x-ray form factors, Compton profiles, and optical conductivity. Our theoretical calculations for Compton profiles and optical conductivity are compared with experimental measurements.^{8,9} (3) Due to the recent advancement in the technology of epitaxial films,¹⁰ there has been intense interest in the subject of magnetic phase transitions of transition metals at lattice constants which are different from the equilibrium one.¹¹⁻¹⁴ We did a series of spin-polarized calculations for lattice constants ranging from 7.0 to 10.0 a.u. Our calculations agree with recent predictions by Moruzzi *et al.*¹⁴ and Fritsche *et al.*¹⁵ that fcc Pd should become ferromagnetic at expanded lattice constants.

II. METHOD

Our calculations employ the LCGO method and the program BNDPKG, which is described in detail in Ref. 16. This method has been applied to many cubic crystals including, recently, the $4d$ transition metals Nb, Mo, and Rh.¹¹⁻¹³ These are all-electron, fully self-consistent calculations. No shape approximations (muffin tins, for ex-

ample) are made concerning the crystal potential. Since the Hamiltonian matrix elements are independent of energy, all eigenvalues are obtained for a given \mathbf{k} with one diagonalization. The principal advantage of the method is that wave functions are obtained in a form which is quite convenient for use in further calculations (the optical conductivity is one example where this can be important). Spin-orbital coupling and other relativistic effects are not included.

Specific aspects of the present calculation include the following: The Gaussian basis set contained 16 s -type, 12 p -type, 8 d -type, and 1 f -type function. The exponents (except for the single f function with an exponent 0.8) were obtained from Ref. 17. The local exchange-correlation potential was of the von Barth Hedin form with parameters determined by Rajagopal *et al.*¹⁸ The iterations leading to self-consistency were based on a grid of 89 points inside $\frac{1}{48}$ of the Brillouin zone. The final band calculation was done on 505 mesh points.

A zero-temperature lattice constant of 7.329 61 a.u., which is extrapolated from the room-temperature value using measured thermal expansion coefficients, is used for the paramagnetic calculations.

III. BAND STRUCTURE AND DENSITY OF STATES

Our calculated bands are shown in Fig. 1. The picture is rather typical for $4d$ transition metals. Strong s - d hybridization is quite evident, particularly along the Δ and Λ directions. There exist several photoemission experiments¹⁹⁻²¹ for Pd(111) in which the band structure is explored along the Λ axis. Judging from the graphic data of these experiments, our calculated band structure is in

reasonably good agreement with the measurements. Numerical results are presented in Table I, where we compare our results with experiment and with other self-consistent theoretical calculations. The degree of agreement between the results of different calculations seems to be superior to that found in Nb and Rh. Here, most level positions agree within about 0.02 Ry. The most significant exception occurs at Γ , where relativistic effects included in the calculation of Ref. 4 lead to a lowering of Γ_1 . The agreement with the experimental results of Ref. 19 is not so good for the lower states at Γ and L , but the serious discrepancies as found in the case of nickel²² are not present here.

The s - d bandwidth defined as $\Gamma_{25'}-\Gamma_1$ is found to be 0.262 Ry while the occupied d -band width measured by E_F-X_1 is 0.4 Ry. In addition to bands listed in Table I, we also found that the gap between band 7 and band 5 at the L point is 8.1 eV, which is in good agreement with the experimental value of 7.8 eV.²¹

The density of states (DOS) is shown in Fig. 2. All major peaks are below the Fermi energy ($E_F = -0.247 04$ Ry). There is a very small peak at 0.26 eV above the Fermi level. The Fermi level is just 0.06 eV above a dominant peak in the DOS. Thus, a relatively large value of the density of states is found at the Fermi level, $D(E_F) = 31.6186 \text{ atom}^{-1} \text{ Ry}^{-1}$. This value is very close to the findings of other calculations. A comparison is given in Table II. Using our value of $D(E_F)$, we obtain a value of $5.41 \text{ mJ mole}^{-1} \text{ deg}^{-2}$ for the electronic specific-heat coefficient γ . The corresponding experimental result by Hoare *et al.*²³ and Chouteau *et al.*²⁴ is about $9.4 \text{ mJ mole}^{-1} \text{ deg}^{-2}$. Hence, we find an enhancement factor of 1.74 which is due to the electron-phonon, electron-

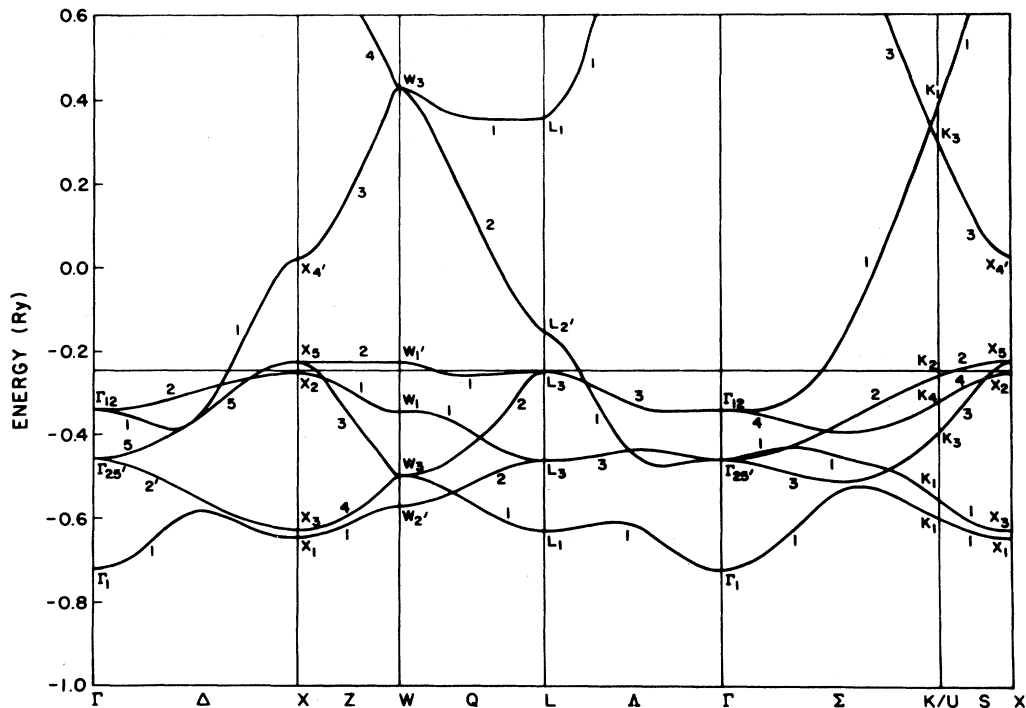


FIG. 1. Energy bands of fcc palladium along symmetry axes.

TABLE I. Comparison of energy eigenvalues at symmetry points. Energies (in Ry) are scaled with respect to the Fermi level. In this work $E_F = -0.24704$ Ry.

	Band 1	Band 2	Band 3	Band 4	Band 5	Band 6
Γ	-0.4733	-0.2111	-0.2111	-0.2111	-0.0927	-0.0927
Γ^a		-0.188±0.011	-0.188±0.011	-0.188±0.011	-0.085±0.007	-0.085±0.007
Γ^b	-0.528	-0.223	-0.223	-0.200	-0.090	-0.090
Γ^c	-0.451	-0.197	-0.197	-0.197	-0.090	-0.090
Γ^d		-0.188	-0.188	-0.188	-0.089	-0.089
X	-0.3985	-0.3803	-0.0005	0.0223	0.0223	0.2260
X^b	-0.400	-0.379	-0.007	0.013	0.034	0.247
X^c	-0.385	-0.353	-0.009	0.020	0.020	
L	-0.3815	-0.2156	-0.2156	-0.0020	-0.0020	0.0921
L^a		-0.176±0.015	-0.176±0.015	-0.029±0.015	-0.007±0.007	
L^b	-0.395	-0.229	-0.204	-0.009	0.005	0.078
L^c	-0.354	-0.204	-0.204	-0.004	-0.004	0.097
L^d		-0.196	-0.196	-0.007	-0.007	
W	-0.3218	-0.2494	-0.2494	-0.0976	0.0225	0.6769
W^b	-0.321	-0.257	-0.249	-0.099	0.021	0.652
W^c	-0.312	-0.229	-0.229	-0.095	0.020	
K	-0.3502	-0.3074	-0.1430	-0.0721	-0.0114	0.5431
K^b	-0.352	-0.309	-0.148	-0.071	-0.012	0.531
K^c	-0.334	-0.289	-0.129	-0.071	-0.011	

^aExperimental values from Ref. 19.

^bRAPW calculations from Ref. 4.

^cKKR results from Ref. 5.

^dMixed basis pseudopotential results from Ref. 6.

electron, and spin fluctuation interactions. In general, features of the DOS found here (such as locations of peaks, the intensity of each peak, etc.) are in good agreement with other calculations.¹⁻⁵ Major peaks of the DOS are found at 4.5, 3.65, 2.57, 2.0, and 1.56 eV below E_F , respectively.

IV. FERMII SURFACE

The Fermi-surface cross sections are shown in Figs. 3(a)–3(c). The surface consists of three sheets: (i) an electron surface around Γ (this is formed by the sixth band); (ii) x -centered hole pockets resulting from the fourth band; and (iii) jungle gym. This sheet consists of the fifth-band hole tubes running along $[100]$ directions. In nonrelativistic calculations, this surface touches the second sheet in the Δ direction. Spin-orbit interaction will split this degeneracy.

In addition to these three surfaces which have been experimentally observed in early de Haas–van Alphen (dHvA) experiments,^{25,26} ultrasonic attenuation²⁷ and more recent dHvA experiments^{28,29} at higher field and lower temperatures revealed a very small (area ~ 0.008

a.u.⁻²) L -centered hole pocket. This L -centered hole surface is not present in the other nonrelativistic KKR calculation⁵ either. Its existence is presumably due to relativistic effects as the spin-orbital interaction will split the degeneracy between band 4 and band 5 along the Λ direction and force band 5 to cross the Fermi surface. Notice that in Table I bands 4 and 5 are only 0.002 Ry below E_F at the L point.

Table III(a) shows three Fermi-surface radii for the Γ -centered electron sheet. These values are compared with the experimental data²³ and other theoretical results.^{2,3}

TABLE II. Density of states at the Fermi level in atom⁻¹ Ry⁻¹.

	$D(E_F)$
Present work	31.6186
Ref. 2	31.06
Ref. 1	32.7
Ref. 4	34.7
Ref. 5	31.4

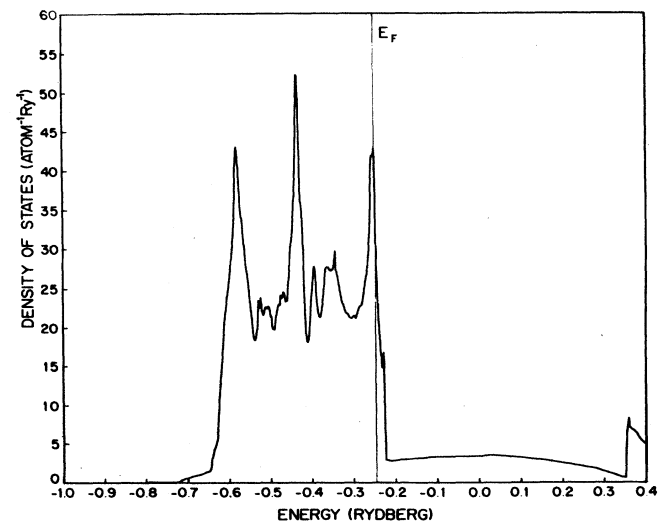


FIG. 2. Density of states of palladium.

TABLE III. (a) Fermi-surface radii for the Γ -centered electron sheet. Units are a.u.⁻¹. (b) Fermi-surface area centered around the X point. Units are a.u.⁻².

Direction	Expt. (Ref. 25)	(a)		
		Present	Ref. 1	Ref. 2
[100]	0.585	0.549	0.578	0.546
[111]	0.593	0.589	0.616	0.568
[110]	0.426	0.415	0.423	0.419

Direction	Expt. (Ref. 28)	(b)	
		Present	Ref. 4
[010] $XW\Gamma$	0.024	0.029	0.021
[100] XWU	0.015	0.013	
[110] $XU\Gamma$	0.024	0.025	0.021

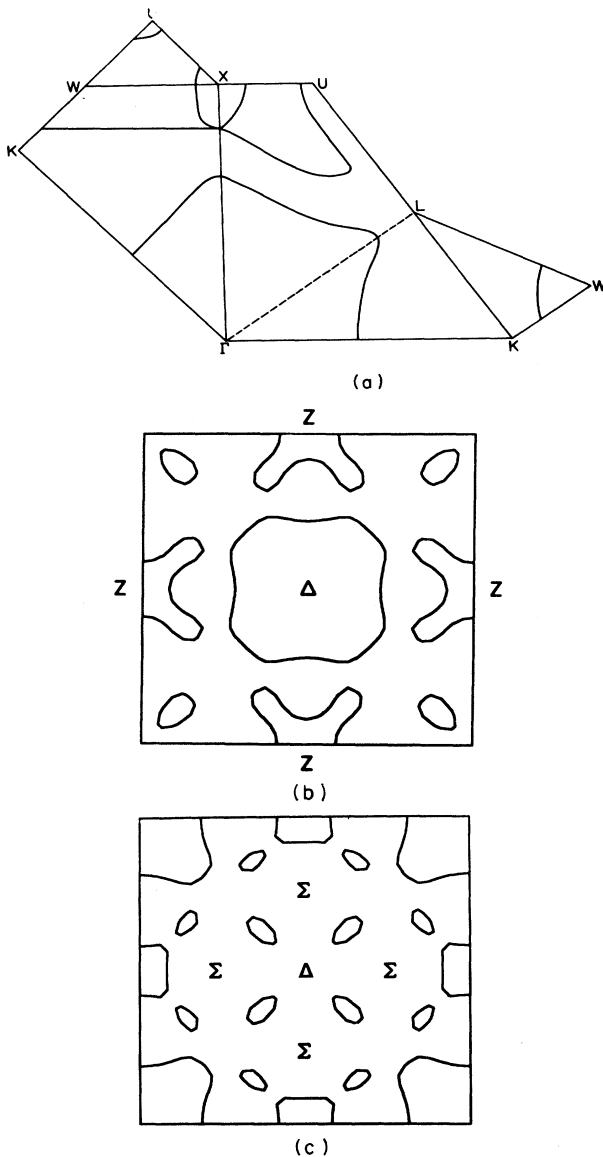


FIG. 3. Fermi-surface profiles of palladium. (a) Unfolded irreducible zone, (b) cross-sectional view in the [001] direction at $[(0.25, 0, 0)(2\pi/a)]$, and (c) cross-sectional view in the [001] direction at $[(0.69, 0, 0)(2\pi/a)]$.

A comparison of the areas centered around the X point is listed in Table III(b). These cross-section areas were estimated by approximating them as ellipsoids. The agreement with experiment is rather good for these cross sections, indicating, as found in many other cases, that local-density-functional calculations can predict the Fermi surface with considerable accuracy.

V. COMPTON PROFILES AND X-RAY FORM FACTOR

Determinations of Compton profiles and x-ray form factors furnish some crucial and sensitive tests on the quality of the bulk wave functions. The Compton profiles of palladium are calculated with the use of the final self-consistent bands. Integrations in k space were performed on a 505-point mesh in $\frac{1}{48}$ of the Brillouin zone in the manner described in Ref. 30. We are not aware of previous calculations of this quantity from self-consistent energy bands (non-self-consistent results have been reported³¹). The core electron contributions have not been included in our calculations.

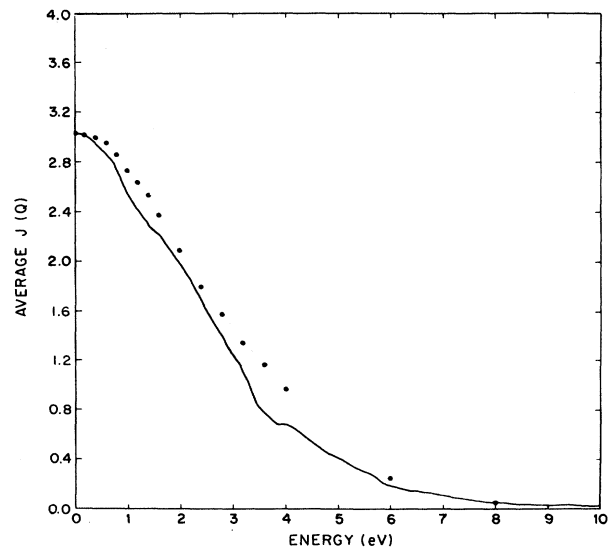


FIG. 4. Spherically averaged Compton profiles for palladium (valence contributions only). Solid line, present calculation; dots, Ref. 8.

Numerical values for $J_{\mathbf{k}}(q)$ (see Ref. 30 for definitions) in the [100], [110], and [111] directions, together with the angular average are given in Table IV. In Fig. 4, the average profile is plotted against the experimental results of Sharma *et al.*⁸ In Ref. 8, some theoretical results were also reported as calculated with the use of the renormalized-free-atom (RFA) model and the APW (non-self-consistent) method. Although the present results are consistently lower than those of Sharma *et al.* for the intermediate values of q , they appear to be superior to the other calculations described. Figure 5 shows our results for the anisotropy of the profile. We are not aware of any experimental measurements on these anisotropic effects.

The calculated x-ray form factors are listed in Table V. Comparing with the free-atom form factors also listed in Table V, we see that the x-ray form factors in the solid are modified only slightly. The bulk value is usually

TABLE IV. Compton profiles for palladium (valence contributions only).

Q (Ry)	[100]	[110]	[111]	Average
0.00	3.066	3.073	2.936	3.035
0.05	3.064	3.060	2.936	3.029
0.10	3.047	3.037	2.938	3.014
0.15	3.012	3.007	2.932	2.989
0.20	2.969	2.967	2.898	2.950
0.25	2.920	2.924	2.855	2.905
0.30	2.882	2.877	2.827	2.865
0.35	2.833	2.818	2.786	2.814
0.40	2.764	2.708	2.724	2.728
0.45	2.692	2.581	2.657	2.632
0.50	2.617	2.456	2.591	2.536
0.55	2.537	2.402	2.523	2.472
0.60	2.460	2.349	2.460	2.409
0.65	2.400	2.292	2.400	2.350
0.70	2.352	2.232	2.333	2.293
0.75	2.301	2.199	2.280	2.249
0.80	2.235	2.179	2.233	2.209
0.85	2.158	2.156	2.184	2.164
0.90	2.077	2.112	2.127	2.106
0.95	1.988	2.071	2.066	2.046
1.00	1.890	2.032	2.003	1.984
1.10	1.725	1.908	1.863	1.844
1.20	1.634	1.717	1.671	1.681
1.30	1.504	1.567	1.492	1.530
1.40	1.343	1.435	1.362	1.390
1.50	1.164	1.299	1.229	1.243
1.60	1.063	1.139	1.104	1.108
1.70	0.946	0.837	0.939	0.894
1.80	0.851	0.697	0.848	0.780
1.90	0.768	0.621	0.762	0.699
2.00	0.711	0.650	0.686	0.677
2.20	0.565	0.590	0.547	0.572
2.40	0.431	0.468	0.445	0.452
2.60	0.334	0.385	0.351	0.362
2.80	0.266	0.303	0.264	0.282
3.00	0.212	0.153	0.202	0.182
3.50	0.099	0.107	0.100	0.102
4.00	0.053	0.056	0.051	0.054
5.00	0.020	0.021	0.021	0.021

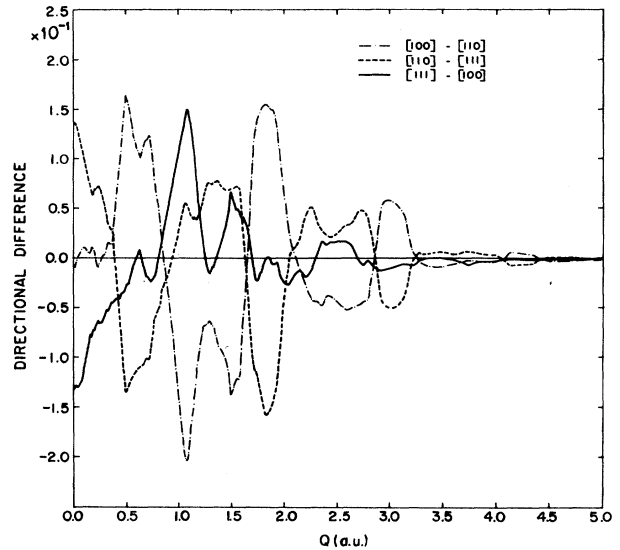


FIG. 5. Anisotropy of calculated Compton profiles.

smaller than the corresponding free atomic value because the wave function in the solid is more extended. Again, we are not aware of experimental results.

VI. OPTICAL CONDUCTIVITY

The optical properties of palladium have been measured by several groups,^{32-35,8} and a brief summary of experimental results was given by Weaver in Ref. 36. It was found that all experiments agree with each other within an uncertainty factor of about 2. These experiments give collectively a rather full picture of the positions of the main anomalies of the imaginary part of dielectric function $\epsilon_2(\omega)$ with photon energies up to 30 eV. Theoretically, Christensen³ has calculated the interband optical conductivity in the approximation of constant matrix elements. Using the same kind of approximation, Ray *et al.*³⁷ obtained $\epsilon_2(\omega)$ based on a non-self-consistent KKR band-structure calculation. Another

TABLE V. X-ray form factors for palladium.

h	k	l	Atomic	Solid
0	0	0	46	46
1	1	1	36.499	35.531
2	0	0	34.560	33.598
2	2	0	29.208	28.408
3	1	1	26.629	25.954
2	2	2	25.934	25.271
4	0	0	23.702	23.214
3	3	1	22.433	21.972
4	2	0	22.065	21.952
4	2	2	20.788	20.467
3	3	3	19.987	19.709
5	1	1	19.987	19.758
4	4	0	18.852	18.691
5	3	1	18.256	18.159
4	4	2	18.069	17.976
6	0	0	18.069	18.025

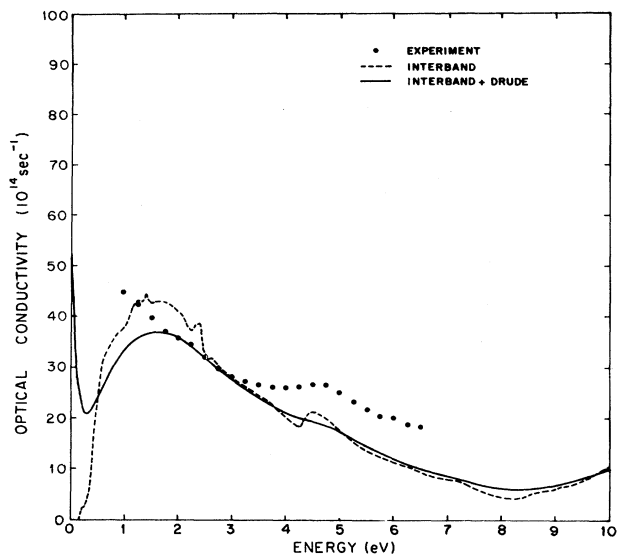


FIG. 6. Optical conductivity of palladium. Dots are experimental data from Ref. 9.

dielectric-function calculation is due to Uspenski *et al.*,³⁸ who used the linear combination of muffin-tin orbitals (LMTO) method. They have computed the matrix elements explicitly. The wave function used in their calculations, however, involves the atomic sphere approximation (ASA).

We have calculated the frequency-dependent interband optical conductivity by integration over the Brillouin zone. The formula for this is standard, and is given in many places.³⁹ The momentum matrix elements are evaluated analytically, as it is quite straightforward to evaluate these matrix elements using a basis of Gaussian orbitals. The results are shown by the dashed curve in Fig. 6. The dotted line is the experimental results reproduced from the graphic data of Johnson and Christy.⁸ The experimental data show structures at about 4.8 and 2.3 eV, which correspond well with our calculations. Additional features of our theoretical results are peaks at 1.2, 1.4, 1.6, 2.4, and 2.6 eV, and shoulders at 0.9 and 7.2 eV. The solid line in Fig. 6 represents the interband plus the Drude optical conductivity. The Drude parameters ($\sigma_0 = 4.0 \times 10^{15} \text{ sec}^{-1}$ and $\tau' = 6.72 \times 10^{-15} \text{ sec}$) were obtained from Lenham and Treherne.⁴⁰

VII. MAGNETIC PHASE TRANSITION

Although fcc palladium is nonmagnetic at the equilibrium lattice constant, one still expects that Pd might become magnetic at a different lattice constant since the degree of *s-d* hybridization usually depends on the lattice constant very sensitively. The fact that Ni (isoelectronic to Pd) is ferromagnetic with a moment $0.6 \mu_B$ also encourages such an expectation. It is therefore an interesting question to see if there exists a range of lattice constants in which Pd is magnetic. We did a series of spin-polarized calculations at various lattice constants to search for this magnetic phase transition. Table VI gives the calculated magnetic moments for Pd at different lat-

TABLE VI. Magnetic moments for different lattice constants.

Lattice constant (a.u.)	Magnetic moment (μ_B)
7.35	0.0
7.50	0.0
7.72	0.0
7.735	0.310
7.75	0.322
7.78	0.334
7.84	0.346
8.00	0.350
8.40	0.336
9.00	0.313
10.0	0.275

tice constants. These results are shown graphically in Fig. 7. A sudden phase transition from a nonmagnetic to a ferromagnetic state occurs when the lattice constant is about 7.735 a.u., which corresponds to a 5.5% increase in the lattice constant beyond the equilibrium value. At a lattice constant of about 8.0 a.u., the system reaches the maximum moment per atom, which is about $0.35 \mu_B$. The magnetic moment then decreases as the lattice constant increases. The moment for Pd in the atomic limit is zero.

Previously, Fritsche *et al.*¹⁵ and Moruzzi *et al.*¹⁴ have investigated this magnetic phase transition for palladium. They found that Pd became magnetic when the lattice constant was expanded by 5 to 6% (10% when the spin-orbital interaction was included). Their results are in excellent agreement with ours. However, we wish to point out that neither the previous calculations nor the current one has considered the possibility of antiferromagnetic ordering. The reason we think Pd may become ferromagnetic is due to the comparison with Ni which has the same lattice structure and the same number of valence electrons. Additional *q*-dependent susceptibility calculations or more direct total-energy calculations including the antiferromagnetically ordered phases are required to clarify this problem.

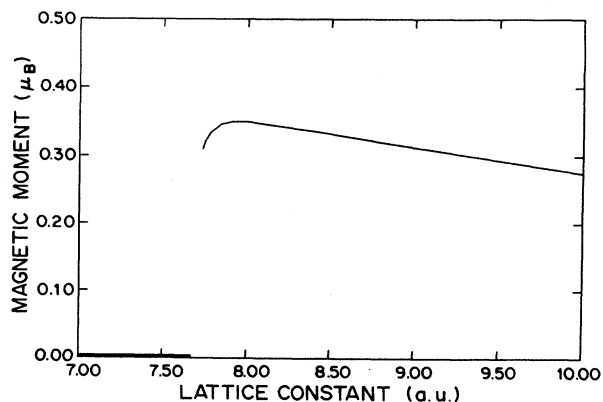


FIG. 7. Ferromagnetic moment of fcc Pd vs lattice constant.

VIII. CONCLUSION

We have calculated the electronic structure of Pd by the LCGO method using the local-density-functional approximation. A variety of properties for fcc Pd have been obtained from our band-structure calculations. In general, our results are in good agreement with available experiments and previous calculations. The most important exception is that the *L*-centered hole pocket is not present in our calculated Fermi surface. This is not unex-

pected since the current work has not included relativistic effects. Additional spin-polarized band-structure calculations were performed at a number of lattice constants. A magnetically ordered phase was found at lattice constants greater than 7.735 a.u.

ACKNOWLEDGMENTS

This work was supported in part by the National Science Foundation under Grant No. DMR-8810249.

-
- ¹O. K. Anderson, Phys. Rev. B **2**, 883 (1970).
²F. M. Mueller, A. J. Freeman, J. D. Dimmock, and A. M. Furdyna, Phys. Rev. B **1**, 4617 (1970).
³N. E. Christensen, Phys. Rev. B **14**, 3446 (1976).
⁴A. H. MacDonald, J. M. Daams, S. H. Vosko, and D. D. Koelling, Phys. Rev. B **23**, 6377 (1981).
⁵V. L. Moruzzi, J. F. Frank, and A. R. Williams, *Calculated Electronic Properties of Metals* (Pergamon, New York, 1978).
⁶S. G. Louie, K. M. Ho, and M. L. Cohen, Phys. Rev. B **19**, 1774 (1979).
⁷J. W. Davenport, Phys. Rev. B **29**, 2896 (1984).
⁸B. K. Sharma, A. Gupta, H. Singh, S. Perkio, A. Kshirsagar, and D. G. Kanhere, Phys. Rev. B **37**, 6821 (1988).
⁹P. D. Johnson and R. W. Christy, Phys. Rev. B **9**, 5056 (1974).
¹⁰G. A. Prinz, Phys. Rev. Lett. **54**, 1051 (1985).
¹¹G. Fuster, N. E. Brener, J. Callaway, J. L. Fry, Y. Z. Zhao, and D. A. Papaconstantopoulos, Phys. Rev. B **38**, 423 (1988).
¹²G. S. Tripathi, N. E. Brener, and J. Callaway, Phys. Rev. B **38**, 10454 (1988).
¹³A. R. Jani, N. E. Brener, and J. Callaway, Phys. Rev. B **38**, 9425 (1988).
¹⁴V. L. Moruzzi and P. M. Marcus, Phys. Rev. B **39**, 471 (1989).
¹⁵L. Fritsche, J. Noffke, and H. Eckardt, J. Phys. F **17**, 943 (1987).
¹⁶C. S. Wang and J. Callaway, Comp. Phys. Commun. **14**, 327 (1978).
¹⁷R. Poirior, R. Kari, and I. G. Csizmadia, Phys. Sci. Data **34**, 9485 (1985).
¹⁸A. K. Rajagopal, S. P. Singhal, and J. Kimball (unpublished), as quoted by A. K. Rajagopal, in *Advances in Chemical Physics*, edited by G. I. Prigogine and S. A. Rice (Wiley, New York, 1979), Vol. 41, p. 59.
¹⁹F. J. Himpsel and D. E. Eastman, Phys. Rev. B **18**, 5236 (1978).
²⁰R. Hora and M. Scheffler, Phys. Rev. B **29**, 692 (1984).
²¹B. Schmiedeskamp, B. Kessler, N. Muller, G. Schonhense, and U. Heizmann, Solid State Commun. **65**, 665 (1988).
²²F. J. Himpsel, J. A. Knapp, and D. E. Eastman, Phys. Rev. B **19**, 2919 (1979); W. Eberhardt and E. W. Plummer, *ibid.* **21**, 3245 (1980).
²³F. E. Hoare and B. Yates, Proc. R. Soc. (London) Ser. A **240**, 42 (1957).
²⁴G. Chouteau, R. Fourneaux, K. Gobrecht, and R. Tournier, Phys. Rev. Lett. **20**, 193 (1968).
²⁵L. R. Windmiller, J. B. Ketterson, and S. Hornfeldt, J. Appl. Phys. **40**, 1291 (1969).
²⁶J. J. Vuillemin, Phys. Rev. **144**, 396 (1966).
²⁷C. R. Brown, J. P. Kalejs, F. D. Manchester, and J. M. Perz, Phys. Rev. B **6**, 4458 (1972).
²⁸D. H. Dye, S. A. Cambell, G. W. Crabtree, J. B. Ketterson, N. B. Sundersara, and J. J. Vuillemin, Phys. Rev. B **23**, 462 (1981).
²⁹W. Joss, L. N. Hall, G. W. Crabtree, and J. J. Vuillemin, Phys. Rev. B **8**, 5139 (1984).
³⁰J. Rath, C. S. Wang, R. A. Tawil, and J. Callaway, Phys. Rev. B **8**, 5139 (1973).
³¹A. Harmalkar, D. G. Kanhere, and R. M. Singru, Phys. Rev. B **31**, 6415 (1985).
³²S. Robin, in *Optical Properties and Electronic Structure of Metals and Alloys*, edited by F. Abeles (North-Holland, Amsterdam, 1966), p. 202.
³³A. Y-C. Yu and W. E. Spicer, Phys. Rev. **169**, 497 (1968).
³⁴R. C. Vehse, E. T. Arakwa, and M. W. William, Phys. Rev. B **1**, 517 (1970).
³⁵S. F. Lin, D. T. Pierce, and W. E. Spicer, Phys. Rev. B **4**, 326 (1971).
³⁶J. W. Weaver, Phys. Rev. B **11**, 1416 (1975).
³⁷N. R. Ray, J. Chowdhuri, and S. Chatterjee, J. Phys. F **12**, 2531 (1982).
³⁸Y. A. Uspenski, E. G. Maksimov, S. N. Rashkeev, and Z. Z. Mazin, Z. Phys. B **53**, 263 (1983).
³⁹For example, see D. G. Laurent, J. Callaway, and C. S. Wang, Phys. Rev. B **20**, 1134 (1979).
⁴⁰A. P. Lenham and D. M. Treherne, in Ref. 32, p. 196.